NITROGEN EXPERIMENTS ON A SUPERSONIC LINEAR CASCADE FOR ORC APPLICATIONS

Marco Manfredi
Energy Department, Politecnico di Milano
Via Lambruschini 4, I-20156, Milano, Italy

Andrea Spinelli
Energy Department, Politecnico di Milano
Via Lambruschini 4, I-20156, Milano, Italy

Giacomo Persico
Energy Department, Politecnico di Milano
Via Lambruschini 4, I-20156, Milano, Italy

Paolo Gaetani
Energy Department, Politecnico di Milano
Via Lambruschini 4, I-20156, Milano, Italy

Vincenzo Dossena
Energy Department, Politecnico di Milano
Via Lambruschini 4, I-20156, Milano, Italy

ABSTRACT

A novel experiment has been conceived at Politecnico di Milano for the study of the flow within and downstream of supersonic cascades of Organic Rankine Cycle (ORC) turbines. This paper documents the first phase of the research, focused on the preliminary tests and studies performed by operating the facility with nitrogen as working fluid, to demonstrate the technical relevance of the experiment and the validity of the measurement system in a simplified thermodynamic condition. The set of measured data includes, beside the inlet total thermodynamic state, eight static pressure values obtained via taps manufactured on the test section rear end-wall, both within the bladed and semi-bladed region of the cascade, as well as a total pressure probe to retrieve the cascade performance. A double-passage Schlieren equipment was also employed to visualize the density gradients. Experiments show an outstanding repeatability and indicate a quasi-steady cascade operation during the blow-down process, especially for the pressure data upstream of the fishtail shocks. Experimental data were also compared with CFD simulations, resulting in an excellent agreement for the pressure data acquired within the cascade, while showing discrepancies in the trailing edge region; such differences are discussed by considering the flow configuration in the trailing edge region, shedding light on the related experimental/numerical issues.

INTRODUCTION

Organic Rankine Cycles (ORC) power systems feature transonic/supersonic turbines, whose design is complicated by the non-ideal thermodynamics of the fluid. Moreover, very few experimental studies on ORC cascades are available in the open literature, due to the technical issues associated to operate, in a laboratory environment, high-speed flows of organic fluids in their plant-relevant conditions, which typically feature relatively high temperature ($\sim 100 - 300\ °C$) and pressure ($\sim 5 - 50\ bar$) as the expansion process starts at conditions close to the critical point of high molecularly complex fluids.

In this context, experiments are further complicated by the need of instrumentation requiring fluid-specific and condition-specific calibration. Consequently, experiments conceived and performed up to date, with the aim of validating CFD tools [1], typically employed simplified flow configurations, such as either isentropic expansions within planar converging-diverging nozzles [2, 3, 4] or supersonic flows over aerodynamic bodies [5]. Such experiments entail the indubitable advantage of providing nearly isentropic flows in large portions of the domain (typically upstream/downstream of shock structures); this greatly simplifies the measurement system, since it allows resorting to measurement techniques, which do not require aerodynamic calibration. In such experiments, upstream total conditions, static pressure measurements along the expansion and schlieren visualization techniques are normally sufficient to characterize the flow. Also optical velocimetry techniques can be applied, though considerably challenging in such flow environment (see [6]).

Despite being relevant for canonical flow characterization and for the development of measurement techniques capable of operating at high temperature, pressure, and with possibly condensing vapors, their relevance for turbine applications is only limited since, without blade rows, wakes, semi-bladed regions, trailing edge structures, crucial loss mechanisms are not reproduced. For this reason, cascade experiments were implemented in [7], but with very limited resolution in space, limited flow non-ideality, and loss evaluation requiring CFD simulations.

In order to fill the current gap in experiments relevant for ORC turbine applications a supersonic linear blade cascade experiment was conceived at Politecnico di Milano on the TROVA facility (Test Rig For Organic VApors) [8] and preliminary tests were performed with nitrogen as working fluid to simplify the interpretation of initial results. The experiments feature a considerably high spatial resolution and allow for a direct evaluation of losses, with no need of CFD simulation other than for comparison reason.

DESIGN OF EXPERIMENT OVERVIEW

The experimental campaign here described was conceived to characterize the flowfield resulting from the expansion of an organic compound (the siloxane MM) in non-ideal thermodynamic conditions through a supersonic turbine linear cascade, including the estimate of the associated total pressure losses. The cascade geometry was therefore designed to simulate the aerodynamics and loss mechanisms of typical supersonic stators implemented in ORC radial and axial turbines. The construction of an appropriate set of measurement techniques is a key feature of the experiment, since the adoption of standard instrumentation requiring calibration is critical when using non-conventional fluids. Moreover, all these requirements needed to comply with the constraints of the experimental facility, such as the size of the test section and the transient operation typical of blow-down wind tunnels (a detailed description of the TROVA facility and of its operation can be found in [2, 8]). Preparatory tests with nitrogen, whose results are discussed in this paper, were carried out to assess the effectiveness of cascade design and of the adopted measurement techniques, since the execution of a single test run is much faster and easier exploiting nitrogen as working fluid.

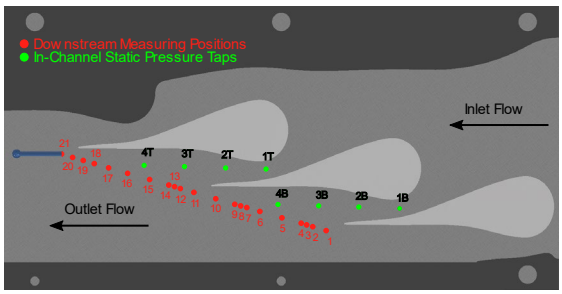

Figure 1: Final test section arrangement together with downstream measuring positions (red dots) and in-channel pressure taps (green dots).

The final cascade arrangement is reported in Figure 1, together with the total pressure probe (sketched in blue), the total pressure measuring grid (red dots) and the in-channel static pressure taps (green dots). The test section features a linear cascade with a geometric pitch of 45 mm, a stagger angle αs = 75°, and composed by three converging-diverging blades, defining two central channels, and two side-walls integrating partial profiles. As clarified in Figure 1, the flow does not undergo any deflection expanding through the cascade, which is characterized by inlet and outlet parallel flows. This choice greatly simplifies the cascade integration within the TROVA test section and makes the cascade representative of both radial-inflow and axial-flow supersonic nozzles. Although the latter are characterized by large deflection, the flow turning is mainly completed upstream the throat, while most of entropy production and blade loading occur in the nearly-straight diverging section of the channel, where the flow is supersonic. This was also confirmed by a dedicated analysis reported in [9], whose results show that the flow rotation upstream the throat does not affect the downstream flow-field topology, as long as supersonic flows are established.

As thoroughly described in [9], the blade and side-walls were designed considering MM as operating fluid and exploiting CFD simulations in order to maximize the periodicity between adjacent channels and to minimize disturbances in the measuring region. The final step of this design procedure consisted into the simulation of the fully 3D domain and of the 2D midspan section of the actual cascade layout. The Mach number field resulting from the 2D computation is reported in Figure 2, highlighting a good periodicity downstream the cascade. Such distribution and the corresponding total pressure field were also exploited to define the spatial resolution and position of the total pressure measuring points reported in Figure 1, which result non-uniformly spaced and conveniently refined in the vicinity of the wakes where higher gradients are expected.

Another proof of the attained periodicity is reported in Figure 3, which depicts the position of the measuring points (vertical dashed lines) along with the Mach distribution at the cascade midspan over the measuring line (black line in Figure 2) versus the non-dimensional pitch-wise distance x_s from the bottom blade trailing edge, for 2D and 3D simulations as well as for design and off-design conditions. For further details concerning the cascade design the reader is referred to [9].

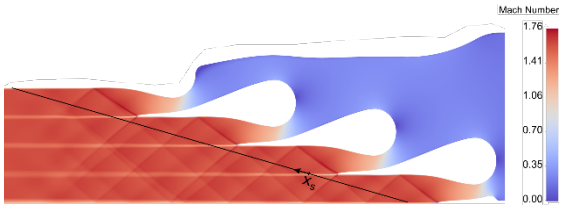

Figure 2: 2D numerical simulation of the actual cascade midspan section: resulting Mach field and measuring locus (black line).

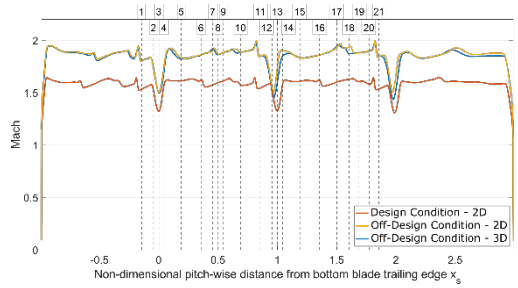

Figure 3: Measuring points positions (black dashed lines) and Mach distribution at midspan section over the measuring.

Since the characterization of the supersonic flow established through the cascade and the estimation of total pressure losses are the primary objectives of the experimental campaigns with both MM and Nitrogen, tailored measurement techniques and a suitable instrumentation have been set-up. Inlet total pressure and temperature are measured in a settling chamber upstream the test section (plenum), in which the flow is smoothly and moderately accelerated such that it has a negligible kinetic energy and can be considered uniform at the cascade inlet. The total temperature is provided through 2 thermocouples (of J and K type) with expanded uncertainty of 1°C. while total pressure is retrieved by a wall flush-mounted absolute piezo-resistive transducer for high-temperature applications with expanded uncertainty of approximately 0.1% of the full scale. All the pressure signals described in the following were measured through such kind of transducers, either flush-mounted or connected through a pneumatic line, each one characterized by a different full scale value. Eight static pressure taps of 0.3 mm diameter were manufactured on the test section rear end-wall, along the center-lines of the diverging region for the two central channels of the cascade (green dots in Figure 1), complemented by an equal number of pressure transducers. The processed signals acquired by these sensors allow to characterize the flow expansion through the diverging nozzle and in the semi-bladed region, both upstream and downstream the fishtail shock stemming from the blade trailing edge. Moreover, they provide a quantitative estimation of the in-channel attained periodicity for different inlet conditions as the test proceeds on.

To measure the total pressure of the flow at the cascade exit, a total pressure probe was applied and a dedicated measurement procedure was conceived. A direct measure of the total pressure downstream the cascade is, indeed, not possible, due to the formation of a detached bowed shock in front of the probe head, the flow outgoing the cascade being supersonic. Moreover, a standard instrument calibrated in advance (such as a 3-hole probe) cannot be directly applied in non-ideal flows, as a dedicated tunnel for non-ideal calibration would be required. The total pressure downstream the cascade – i.e. the one upstream the probe-induced shock – can be indirectly retrieved by applying normal shock relations in combination to the total pressure measured by the probe (sketched in blue in Figure 1) and the wall static pressure measured upstream of the shock. The latter is provided by a pressure tap machined in the in the rear end-wall plate exactly below the total pressure probe head tip. In fact, the wall pressure measured in this point is fully representative of the static pressure upstream the shock, as proven by analyses based on Moeckel's theory [10] and on high-fidelity CFD computations, whose description lies outside the scope of the present paper. The total pressure probe features a recessed stem and a 15 mm long head, it is pre-aligned with the flow and located at the test section mid-span, and it is linked to the corresponding pressure transducer by means of a pneumatic line system. To ensure structural stiffness and to withstand high-pressure loads, a probe made by cobalt-chrome alloy and manufactured by means of stereolithography was considered. In this way the probe did not exhibit any stem oscillations or deformations independently on the inlet conditions investigated (up to 25 bar). A probe external diameter of 1.6 mm was chosen as a compromise between spatial resolution and instrument stiffness, while the internal diameter was set equal to 1 mm. This choice resulted from a trade-off between minimizing the integration area and ensuring a pneumatic line system dynamic response fast enough to follow the vessel emptying process as the test proceeds on. To characterize the total pressure loss pitch-wise distribution along the two central channels, a traversing system made up of 21 measuring points not uniformly spaced was devised (red dots in Figure 1). Since the facility is operated with a blow-down approach and a limited number of access points are available, one single measuring position is investigated during a single test, making the probe traversing possible only by combining multiple test runs. This choice is justified by an already proven test repeatability [11].

Finally, a double-passage Schlieren equipment was also employed to visualize the flow-field density gradients. This allows characterizing with almost continuous space resolution the structures of fan/shock waves developing in the diverging part of the channels and at the blade trailing edges, as well as the shape of the probe-induced shock and the number and direction of the shock waves reflected at the bottom side-wall.

NITROGEN EXPERIMENTS AND RESULTS

Experiments in Nitrogen were carried out to assess the effectiveness of the designed cascade in reproducing the flow field of actual supersonic turbine stators, both in terms of expansion-fan and shock-wave patterns and of cascade periodicity.

Moreover, such experiments were also useful to test the instrumentation and the measurement technique conceived for computing total pressure losses from acquired pressure signals. A total number of 22 tests were performed to investigate different configurations, in which the total pressure probe is either absent or placed in a limited number of downstream measuring points (holes 1, 6, 11, 16, and 21 in Figure 1). Experiments without the probe are of outstanding importance to assess and characterize the flow morphology, including the several configurations of fan/shock waves, without the disturbances arising from the introduction of a solid body (the probe) in a supersonic flow. Most of the experiments where carried with an upstream total pressure of 10 bar, with only some of them featuring 5 bar or 15 bar to assess for any unexpected difference in the flow field produced by a variation of the inlet total pressure. The pressure signals and the Schlieren videos acquired from Nitrogen experimental campaign were mainly used to assess three important features: repeatability of tests with and without the probe, fluid-dynamic periodicity among the two central channels, and agreement of experimental data to CFD results.

To confirm the experiments repeatability is unavoidable since the characterization of total-pressure pitch-wise distribution relies on this assumption, the latter being constructed by combining different tests. Since an accurate control of total pressure at the test section inlet is not possible, only similar values can be warranted between two different tests, with an accuracy of about $\pm$ 0.5 bar. This characteristic of the facility makes meaningless the comparison of acquired pressure signals from different experiments as function of time. More relevant insights may be instead obtained comparing the ratios between the acquired pressures and the total inlet total pressure P_{T0} as function of a suitable non-dimensional value of the inlet total pressure itself P_{Tr}, defined as

$$P_{T,r} = \frac{P_{T0,max} - P_{T0}}{P_{T0,max} - P_{T0,min}},$$

where $P_{T0,max}$ and $P_{T0,min}$ are , respectively, the maximum and minimum values of the inlet total pressure P_{t0} occurring during each test run. First of all, to verify the signals repeatability for the 8 in-channel static pressure taps (labelled green dots in Figure 1) 3 experiments without the total pressure probe were considered, in the following referred to as TNP1, TNP2, and TNP3. The results in terms of pressure ratios against non-dimensional total pressure $P_{T,r}$ are reported in Figure 4.

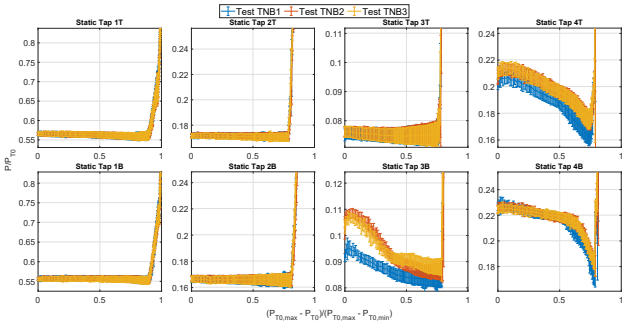

Figure 4: Comparison of static pressure signals acquired by in-channel taps for 3 different tests without total pressure probe. Note that the pressure signals rise considerably at the end of the experiment due to a rise in the backpressure of the facility, which pulls the shocks upstream and within the bladed region

From left to right, data are ordered from the most upstream to the most downstream tap, having in the first row the signals from the upper channel. The pressure ratios retrieved from positions 1T, 2T, 3T, 1B, and 2B are not only perfectly overlapped, indicating an outstanding repeatability, but they are also constant as the test proceeds on and the inlet total pressure decreases ($P_{T,r} \rightarrow 1$). In fact, these pressure taps are located along the centerline of the diverging part of the 2 central channels, upstream the fishtail shock originating from the blade trailing edges, as shown in Figure 5, in which a Schlieren frame from test TNP2 is reported. In this region an almost isentropic flow is established, resembling the flow-field through converging-diverging nozzles, in which the value of P/P_{T0} does not depend on the absolute values of P_{T0} but only on the geometrical area ratio.

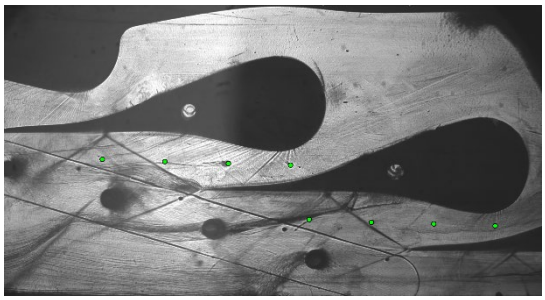

Figure 5: Frame from a schlieren visualization of a nitrogen test without the probe (TNP2)

Figure 5 helps also to explain the differences between the pressures acquired by taps 3T and 3B, the latter being characterized by different signals from the 3 experiments and consequently by a misleading poor repeatability. In fact, due to a non-perfect periodicity (iscussed in detail below), in the upper channel the fishtail shock impinging on the pressure side of the blade lies just downstream the third tap (tap 3T), while in the lower channel this shock is exactly overlapped to the third tap (3B). This situation justifies the limited scattering of the pressure acquired by tap 3B among different tests,

being the exact opening of the fishtail apt to slight randomic oscillations. Finally, the pressure signals acquired by taps 4T and 4B present good repeatability and similar descending trends caused by a faster decrease of the static pressure with respect to the inlet total pressure.

To assess the repeatability when the total pressure probe is installed, at least two tests were performed for every downstream measuring position considered (holes 1, 6, 11, 16, and 21 in Figure 1). In particular, the pressure signals acquired in different experiments by the probe and by the static pressure tap placed below the probe head tip were considered and compared. The results of such analysis are reported in Figure 6, where the static and total pressure acquired during tests TP6 and TP21 (probe in position 16 and 21 respectively) are compared with those acquired during the repetitions of those experiments (tests TP6bis and TP21bis). As previously motivated, the ratios between the measured and the inlet total pressure are plotted against the non-dimensional pressure ratio $P_{T,r}$. Figure 6 highlights a good repeatability featuring both the static and total pressure signals, independently on whether measuring position 16 or 21 is considered. Similar results were obtained for the other measuring positions (1, 6, and 11).

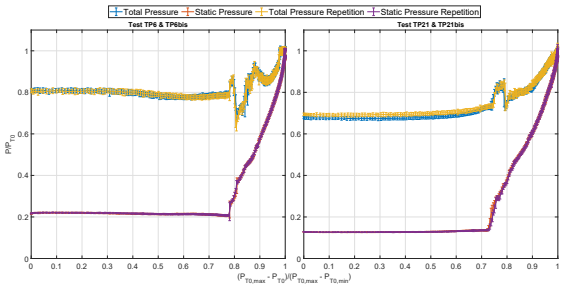

Figure 6: Total and static pressure measurements downstream the cascade for 2 different probe positions (16 and 21) and corresponding test repetitions.

As detailed in Section 2, a primary target of the test section design was to obtain a good periodicity between the two central channels when the cascade is operated with the organic fluid MM. However, it is worthwhile to assess the degree of periodicity also when the selected working flid is Nitrogen. To this end, the experimental data from test TNP2 can be considered since not only the signals from in-channel pressure taps (taps 1T, 2T, 3T, 4T, 1B, 2B, 3B, and 4B) are acquired but also the mid-channel pressures downstream the cascade, at measuring position 6 and 16, are measured. The acquired absolute static pressures are reported in Figure 7 as function of the test running time. Besides providing a direct proof of attained cascade periodicity, this representation is in fact useful to appreciate the emptying dynamics, typical of blow-down wind tunnels, characterized by slowly decreasing pressure levels. The results in Figure 7 highlight a very good periodicity for the two most upstream pressure taps (taps 1T/1B and taps 2T/2B). The pressure signals retrieved downstream the pressure-side fishtail shocks - i.e. taps 4T/4B and measuring positions 16/6 - present similar trends but slightly different absolute values for most of the test duration, highlighting a non-perfect degree of periodicity in the semi-bladed region and downstream the cascade.

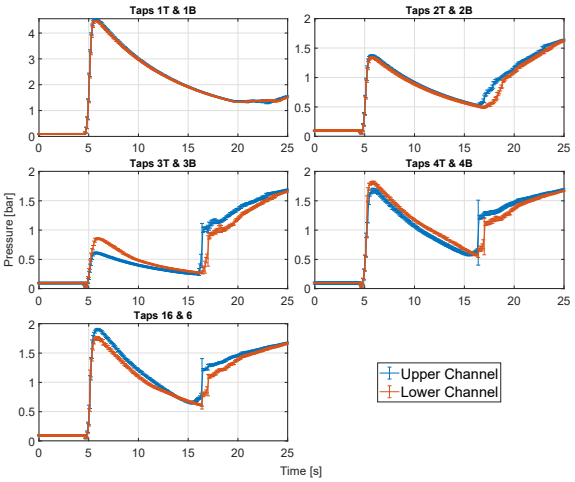

Figure 7: Comparison between upper and lower channels for TNP2: in-channel static pressure taps and measuring positions 16 and 6.

The larger discrepancies between the signals provided by taps 3T and 3B, especially in the first part of the test run, can be explained by a slightly different inclination of the fishtail shocks (especially the ones directed towards the adjacent-blade suction side) caused by a non-perfect periodicity between the two channels. In fact, as previously highlighted, a small rotation of the lower channel fishtail in the upstream-wise direction produces a large increase of the pressure measured since tap 3B is placed very close to the shock, in a region characterized by high pressure gradients. This behavior is confirmed by the trend observable in the second part of the test run, in which the signals acquired by taps 3T and 3B are nearly overlapped. In fact, as confirmed by the Schlieren video, the opening angle of the lower channel fishtail tends to reduce as the experiment proceeds on, leading to a much better periodicity of the signals acquired by taps 3T and 3B.

Experimental data from test TNP2 were also compared with the results of CFD simulations. In particular, a 2D numerical domain representative of the test section midspan was considered, exploiting muti-block structured meshes created with ANSYS-ICEM CFD. Following a dedicated grid-dependence analysis, whose description lies outside the scope of the present paper, a mesh size characterized by 345 thousands cells was chosen. The ANSYS-Fluent solver was used, integrating the RANS equations complemented by the $k-\omega$ SST turbulence model and by look-up tables to introduce the

thermophysical properties of Nitrogen (modelled as non-polytropic ideal gas). To provide a fair comparison with data from test TNP2, numerical simulations were performed by setting the inlet total pressure and temperature equal to those measured in a specific time instant. In particular, the condition of maximum inlet pressure was considered, in which measured inlet total pressure and temperature are $P_{T0} = 8.02$ bar and $T_{T0} = 282.14$ °C respectively. For further details concerning the numerical set-up the reader is referred to [9].

First of all, the Mach number field extracted from the numerical simulation results is compared in Figure 8 with the Schlieren frame corresponding to an inlet total pressure of 8.02 bar. Moreover, in Figure 9 the signals acquired by the in-channel transducers (tap 1T, 2T, 3T, 4T, 1B, 2B, 3B, and 4B) and the downstream static pressures retrieved in positions 6 and 16 at the time instant corresponding to $P_{T0} = 8.02$ bar are compared with the corresponding values resulting from the CFD simulations. The pressure values numerically computed are reported in Figure 9 together with the related error-bars, which take into account the pressure variation over a circle with a radius of 0.3 mm (equal to the one of the manufactured taps). The results reported in Figure 9 clearly highlight an outstanding agreement between experimental and numerical data whenever the pressure taps are within the bladed portion of the channel, namely upstream the fishtail shocks originated from the blade trailing edge (taps 1T, 2T, 3T, 1B, and 2B). Pressure tap 3B presents slightly larger measured values compared to the computed one since, as already discussed and reported in Figures 4 and 7, the fishtail shock in the downstream channel is more rotated upstream, so that the tap 3B results in a region of very high pressure gradients. This situation is particularly evident in the first part of the test running time (it is worthwhile to highlight that the time instant investigated in Figures 8 and 9 is at the beginning of the test, when the maximum inlet total pressure occurs), while after few seconds the downstream fishtail shock rotates downstream.

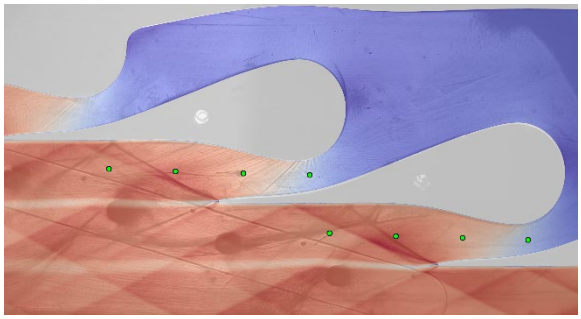

Figure 8: Comparison between schlieren visualization and computed Mach field at same inlet total conditions for TNP2.

This variation of the shock pattern improves the periodicity between the two channels (see middle-left plot of figure 7, after about 10 seconds) and, consequently, greatly reduces the discrepancies between experimental an numerical values for tap 3B. The non-perfect periodicity between the two fishtail shock patterns at the beginning of the test is evident also in Figure 8, in which the Schlieren image is compared to the computed Mach number field. In fact, Figure 8 highlights significant discrepancies between the predicted and experimental fishtail shock patterns, especially in the bottom channel. In particular, the Schlieren-visualized fishtail shocks oriented to the adjacent blade suction sides have a larger opening angle (measured with respect to the axial direction) than those predicted by CFD simulation, suggesting that a stronger recompression takes place through the cascade-exit shocks in the experiments.

This is in coherent with the results reported in Figure 9 for taps 4T and 4B and for measuring positions 6 and 16, which highlight measured pressure values higher than those predicted by numerical simulations.

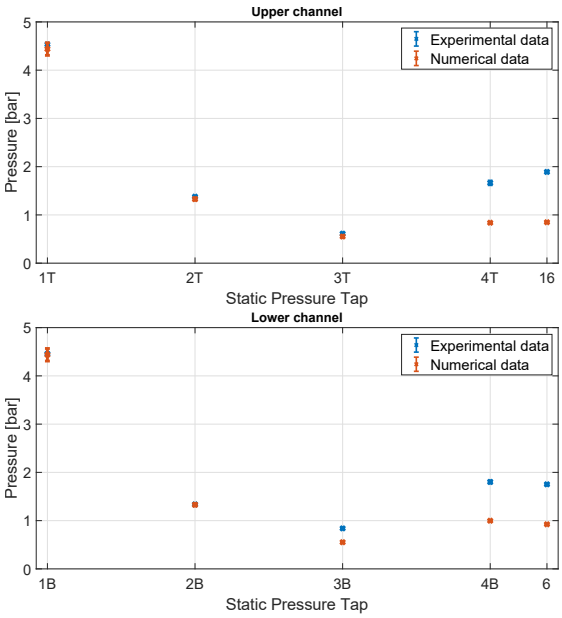

Figure 9: Comparison between measured and numerical static pressures computed at the same total inlet conditions for TNP2: in-channel static pressure taps and measuring positions 16 and 6

Several attempts were made to reduce such discrepancies, either acting on computational aspects related to the geometry (e.g., a 3D flow model and a domain reproducing the exact shape of the test section) or to the numerical set up (modifying the numerical schemes and the turbulence models). However, all the numerical solutions provide roughly the same results without reducing the discrepancies with pressures measured downstream the fishtail shock pattern. It is worthwhile to highlight that also the Schlieren-

visualized suction side fish tail shocks present a different opening angle with respect to those numerically predicted and, in particular, they result more rotated downstream, contrary to what happen for the pressure side fish tail shocks. This implies that experimental fish tail shock patterns appear globally clockwise rotated.

These observations indicate that further investigations are also required on the experimental set-up. Such investigations are presently ongoing and will constitute a new set of data to be presented at the Conference.

CONCLUSIONS

This paper has presented a set of novel experiments on a supersonic linear cascade specifically conceived for experimental studies on ORC turbine nozzles. Due to the specific requirements of operating with organic fluids, and their non-ideal thermodynamics, a dedicated measurement system was developed, which combines static pressure measurements, Schlieren visualizations, and a total pressure probe which does not required aerodynamic calibration. The paper has documented the preliminary assessment of the cascade operating the facility with nitrogen, so to reproduce the correct flow regime (Mach number exceeding 2) while removing the complexity associated to the non-ideal thermodynamics of the fluid.

Experiments showed that pressure data acquired upstream of the cascade opening feature excellent repeatability and periodicity between adjacent channels; instead, pressure data acquired from taps placed in the semi-bladed region exhibited a not perfect periodicity due to the effect of the fishtail shock pattern stemming from the trailing edge. Schlieren visualizations confirm that the flow configuration in the trailing edge region is not perfectly periodic between adjacent channels; this was, however, expected, since the side walls of the cascade were designed to optimize the periodicity when operating with the organic fluid MM.

Measurements were also compared with CFD simulations performed with the same flow model applied to design the cascade. The calculations reproduced in very good approximation the flow configuration within the channel up to the fishtail shock system, but they underestimating the pressure at the cascade exit. Correspondingly, differences in the shock inclination appear in the visualizations, suggesting the onset of a different cascade backpressure between the experiment and the simulation. These observations have led to further experimental investigations, which are presently ongoing and are leading to a set of completely new experiments. This new test campaign will also include total pressure measurements at the cascade exit, leading to an experimental estimate of the cascade loss coefficient.

ACKNOWLEDGMENTS

This research is part of the Energy for Motion project of the Department of Energy of Politecnico di Milano, funded by the Italian Ministry of University and Research (MUR) through the Department of Excellence grant 2018-2022.

REFERENCES

[1] G. Gori, M. Zocca, G Cammi, A. Spinelli, P.M. Congedo. *Accuracy assessment of the Non-Ideal Computational Fluid Dynamics model for siloxane MDM from the open-source SU2 suite.* European Journal of Mechanics, B/Fluids, 79, 109–120 (2020).

[2] A. Spinelli, G. Cammi, S. Gallarini, M. Zocca, F. Cozzi, P. Gaetani, V. Dossena, A. Guardone. *Experimental evidence of non-ideal compressible effects in expanding flow of a high molecular complexity vapor.* Experiments in fluids 59 (2018).

[3] M. Robertson, P. Newton, T. Chen, R. Martinez-Botas. *Development and commissioning of a blowdown facility for dense gas vapours.* In: Proceedings of ASME Turbo Expo, Phoenix, U.S. 2019. GT2019-91609.

[4] F. Beltrame, A. Head, C. De Servi, M. Pini, F. Schrijer, P. Colonna. *First experiments and commissioning of the orchid nozzle test section*. In: ERCOFTAC Series 28 (2021) 169–178.

[5] M. Zocca, A. Guardone, G. Cammi, F. Cozzi, A. Spinelli. *Experimental observation of oblique shock waves in steady non-ideal flows.* Experiments in fluids 60 (2019).

[6] Gallarini, F. Cozzi, A. Spinelli, A. Guardone. *Direct velocity measurements in high-temperature non-ideal vapor flows.* Experiments in Fluids, 62(10), 2021.

[7] D. Baumgärtner, J.J. Otter, A.P.S. Wheeler. *The effect of isentropic exponent on transonic turbine performance.* Journal of Turbomachinery, 142(8), 081007 (2020).

[8] A. Spinelli, M. Pini, V. Dossena, P. Gaetani, F. Casella. *Design, Simulation, and Construction of a Test Rig for Organic Vapors*. Journal of Engineering for Gas Turbines and Power 135 (2013).

[9] Manfredi, M., Persico, G., Spinelli, A., Gaetani, P., & Dossena, V. (2021). *Design of Experiments for Supersonic ORC Nozzles in Linear Cascade Configuration*. In 6th International Seminar on ORC Power Systems (pp. 1-12).

[10] W. E. Moeckel. *Approximate method for predicting form and location of detached shock waves ahead of plane or axially symmetric bodies*. Technical report, 1949.

[11] G. Cammi, C. Conti, A. Spinelli, A. Guardone, *Experimental characterization of nozzle flow expansions of siloxane mm for orc turbines applications*, Energy 218 (2021).